

Technology of fabrication of chalcogenide glassy semiconducting films

V. PRILEPOV, M. POPESCU^{a*}, A. CHIRITA, O. KORSHAK, P. KETRUSH, N. NASEDCHINA

Department of Physics, State University of Moldova, Chisinau, Republic of Moldova

National Institute R& of Materials Physic, Bucharest-Magurele, POB MG.7, Romania

The results of the studies of thin layer structures based on chalcogenide glassy semiconductors (CGS) in As-Se-S system are presented in the paper. The possibility of producing As-Se-S thin films with desired electro-physical properties is shown.

(Received September 1, 2013; accepted November 7, 2013)

Keywords: Chalcogenide glass, Thin films, Technology of production, Material properties

1. Introduction

The investigation of chalcogenides, especially in amorphous state is a subject of current interest [1-9].

The thermal evaporation in the vacuum from the open evaporators is widely used at the fabrication of thin semiconductor layers. The results are considered satisfactory if the physical parameters of the obtained layers are in correlation with the parameters of the given material.

It is well known that (CGS) of $As_2S_{3x}Se_{(1-x)}$ type ($0 \leq x \leq 1$) is an amorphous phase in thin films. In a large range of the technological methods of their fabrication. Such layers are thermally stable, do not interact with the moisture, with the organic solvents and do not reveal any relation between semiconductor bandwidth and the studied composition. The CGS layers having the thickness of 2-4 μm practically always possess a mirror like homogeneous surface and a good adhesion to the substrate. But the structure complexity of CGS glassy state which includes atomic chains, wide rings and bands [10] does not allow fabrication of thin layers with the identical electro-physical parameters by using different methods. Moreover the CGS layers plasticizing is possible by addition of small amounts of ligature as at 5-7% the addition, as a rule, results in the appearance of a crystalline phase, and small concentrations are "smeared" by the absence of the long-range order in the material structure.

This paper is related to the studies of the peculiarities of CGS thin film fabrication, including on to a large extension flexible substrates.

2. Experimental

2.1 Evaporation kinetics of CGS materials based on As-Se-S system

For the studies of evaporation kinetics, the temperature dependence of CGS (W/T.s) was studied, as it is characterized by the amount of the substance evaporated from the surface unit during a time unit, and it is related to the saturated vapors pressure and its molecular composition at the given evaporation temperature (T_{ev}).

Studies of CGS temperature dependence of the evaporation rate the method of the evaporation process evolution in time [11] was followed. A narrow condensation band was established where the layers were deposited on a transparent basis lavesan moving at a constant rate. The mass of CGS portion was constant. The evaporator mass neither more than by 10 times exceeds the mass of downloadable portion, which considerably decreases the time of its heating up, at this constructively the evaporator temperature was fixed from outside. The condensate thickness distribution was estimated by optical transmission (T%) at the wavelengths (λ) from the fundamental absorption region of the corresponding CGS material. As one can see from Fig.1 the evaporation process is not a homogeneous one and depends on the evaporation temperature. The homogeneity of the condensate varies significantly.

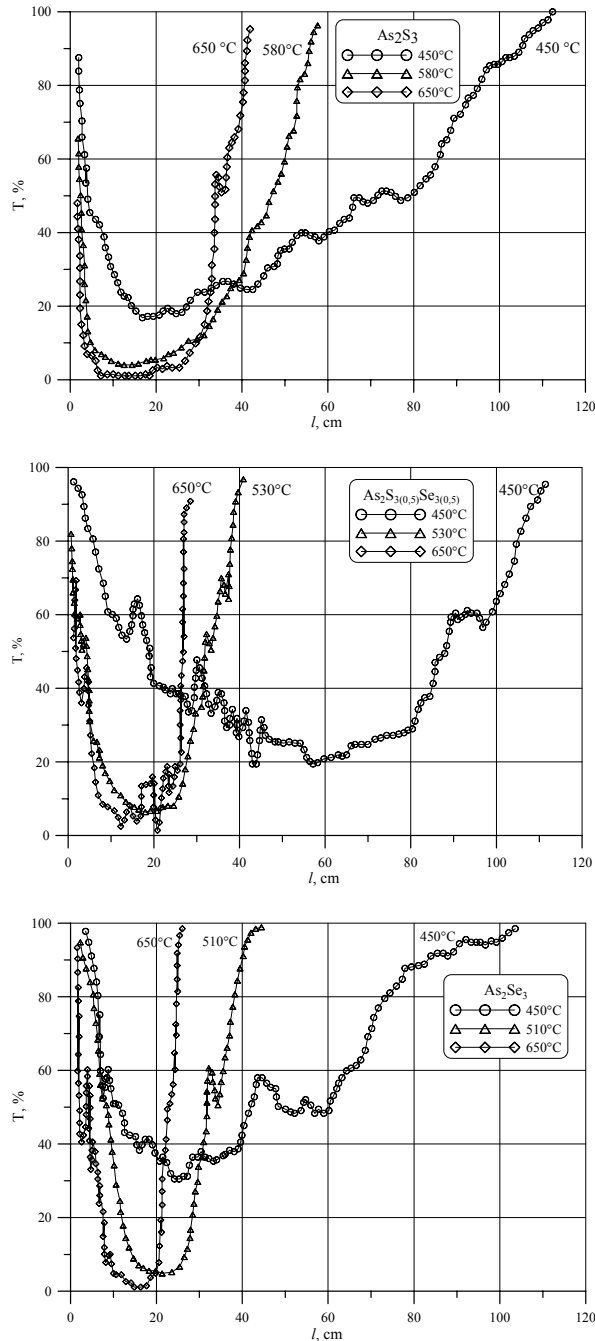


Fig.1. The characteristics of CGS after evaporation process for three different evaporator temperatures.

The condensate inhomogeneity at the initial stages is related to the CGS material supply on to evaporator and its heating up. The inhomogeneities at the final stages is related to the evaporation of the residues and only the middle stage characterizes the peculiarities of the given CGS evaporation. At low and high evaporator temperatures an average CGS evaporation rate does not considerably change (Fig.2).

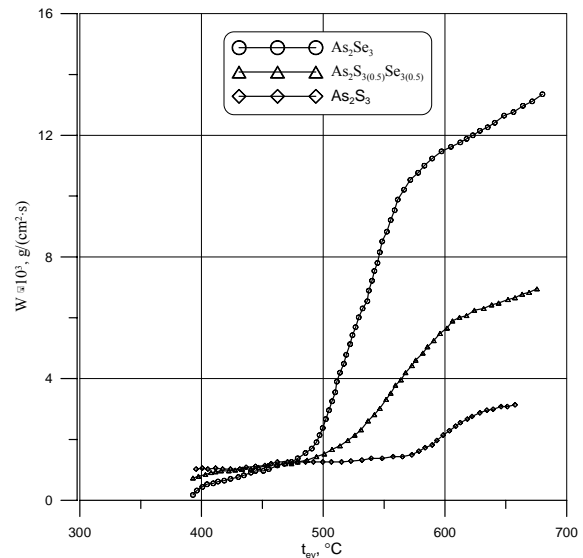


Fig.2. The temperature dependence of average evaporation rate for different CGS compositions

On the transitional segments a sharp $W_{av}=f(T)$ dependence is observed, for which the evaporation feature is homogeneous. The evaporation rate, i.e. the substance amount evaporated from 1cm^2 of the evaporator during 1s, is related to the saturated vapors pressure by the formula:

$$W(T) = 0.0585 \sqrt{\frac{M}{T}} \cdot P(T) \quad (1)$$

Where T - is evaporation temperature, M - evaporated material molar weight, $P(T)$ - the evaporated material saturated vapors pressure which for As_2Se_3 according to [12] is written as :

$$\left. \begin{aligned} \lg P(T) &= -\frac{9092}{T} + 13.4 & 541 < T < 626 \text{ K} \\ \lg P(T) &= -\frac{5683}{T} + 7.9 & 926 < T < 1100 \text{ K} \end{aligned} \right\} \quad (2)$$

The joint solution of (1) and (2) gives the theoretic behavior of As_2Se_3 evaporation rate by time (Fig.2) which corresponds to the experimental data.

At low evaporation temperatures the material in the evaporator is heated up slowly and irregularly due to convective heat transfer, which determines weak variation $W_{av}(T)$ and a considerable irregularity of the condensate. When the evaporator temperature increase the CGS liquid material begins to boil by forming intensive bubbles of saturated vapors, which rises through the material thickness to the surface warm up the CGS and burst by supplying all the temperature set of the saturated vapor to the substrate, what determines the homogeneous condensate composition in the transition area. The critical

radius of the bubble, which could come off from the evaporator bottom on the account of the pull out Archimedes force, by overcoming the liquid As_2Se_3 surface tension, was 2 mm and the temperature of possible appearance of such bubbles is around $410^{\circ}C$. The given temperature corresponds to the initial region of the transition from the first segment to the second one of the $W_{av}(T)$ dependence. Experimentally was established higher transition temperature, which could be explained by the presence of different centers of bubble formation. At high temperatures on the segments of transition to the third region the bubbles have no time to come off from the evaporator walls and merge into a single vapor layer. The material heating up in this case occurs on the account of radiation. By coming from Stefan-Boltzman's equation the calculated temperature of the transition to the third region for As_2Se_3 makes $\approx 540^{\circ}C$, which correlates with the obtained experimental data.

So, for the obtaining of the homogeneous CGS films with a constant and reproducible electro-physical parameters one should use an evaporator of the open type, and the evaporation temperature should ensure the bubble mechanism of CGs warming-up in the evaporator.

2.2 Open type evaporators with an activated surface

From the physics of the liquids boiling it is known [13,14] that for the formation of the gas bubbles at the bubble boiling the cores, let it be of a small but limited dimensions, are needed. Such cores could be the microscopic defects as well as cavities on the solid state surface. For the cavities to act as steady centers of the bubble formation it is necessary the following conditions to be satisfied: vapor penetration inside of the cavity; the dynamic stability of gas-liquid interface inside of the cavity; statistical stability related to the bubbles growth reaching the cavity outlet. The scheme of the stability of three phases (solid state -3, liquid -2, gas -3) stability related to a small drop situated on a solid state surface. One can write:

$$\begin{aligned} \sigma_{SV} - \sigma_{SL} &= \sigma_{LV} \cos \Theta \\ \cos \Theta &= \frac{\sigma_{SV} - \sigma_{SL}}{\sigma_{LV}} \end{aligned} \quad (3)$$

where σ_{sv} is the surface tension between solid state and gas, σ_{sl} is the surface tension between liquid and gas, Θ - is wetting contact angle.

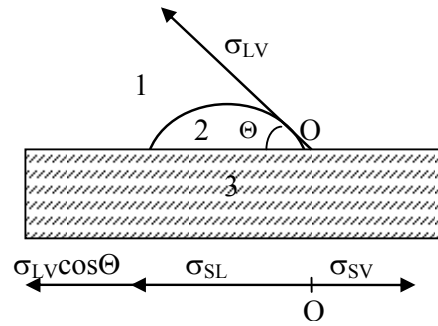


Fig.3 Stability at the three phases interface: gas- 1, liquid- 2, solid state -3.

Though it is impossible independently to change the liquid surface tension σ_{lv} , nevertheless at σ_{lv} increase the contact angle increases and the surface is worse wetted by the liquid, at this the time of surface release from the bubble increases too. To accommodate the cavity stability on the warm up surface acting as center of the bubble generation, let us consider the characteristic of the vapor volume, captured by a conical cavity (Fig.4).

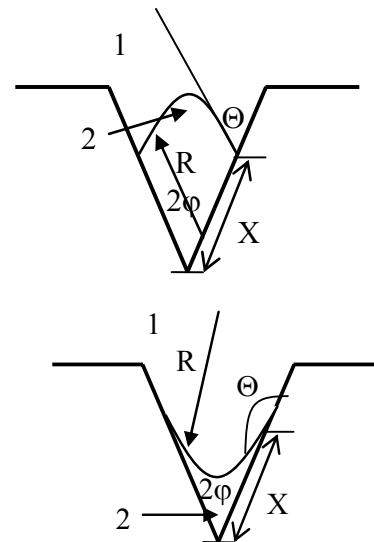


Fig.4. Statistical stability of a cavity: 1- liquid, 2- vapor; (a)- good wetting $\Theta < \frac{\pi}{2} + \varphi$; (b) $\Theta > \frac{\pi}{2} + \varphi$.

The angle on the cavity top is 2φ , the contact angle is Θ . In this case the curvature radius R of the gas – liquid interface takes the form:

$$R = \frac{\sin \varphi}{\sin\left(\Theta - \varphi \pm \frac{\pi}{2}\right)} \cdot X; \quad (+): \Theta < \frac{\pi}{2} + \varphi \quad (a)$$

$$(-): \Theta > \frac{\pi}{2} + \varphi \quad (b)$$

$$(4)$$

Where, X- is the generatrix length of the conical surface. In both cases the coefficient at X in the right side is positive.

The vapor pressure inside cavity, P_V , could be represented by the curvature radius and by the liquid pressure on cavity P_∞

$$P_V = P_\infty \pm \frac{2\sigma_{LV}}{R}; \quad (+): \Theta < \frac{\pi}{2} + \varphi \quad (a)$$

$$(-): \Theta > \frac{\pi}{2} + \varphi \quad (b)$$

$$(5)$$

In the case represented in Fig.4a or at low values of the length X, the vapor pressure increases and the corresponding saturation temperature increases too. If this temperature will be higher than of the vapor main volume local part, then in the vapor volume a hidden heat is released and the condensation occurs. As a result the vapor volume decreases and this process will repeat until the thermodynamic stability between gas and liquid comes. In the case represented in Fig.4b the pressure inside of the vapor volume will decrease and the corresponding saturation temperature decreases, as a result the stability corresponding to the pressure P_V is reached. If the liquid surface tension σ_{lv} is high or the surface tension at the solid state-vapor σ_{sv} or when both of the above conditions are performed then the contact angle Θ (formula 3) will increase and the vapor volume captured by the cavity stabilizes. Thus the stabilization of the bubbles formation centers occurs. The simplest method of cavities stabilization on the evaporator surface is the using of the heating up surface with a low free energy or is sufficient to decrease the surface free energy of the inner walls of the cavities.

The open type evaporators made from stainless steel or tantalum proved to be reliable devices for CGS layers fabrication due to their good wetting by the evaporated material, to the absence of its perceptible interaction with the evaporator material, to the simplicity and reliability of the design.

For the decrease of the metallic evaporator surface free energy it was suggested [15] to activate their surface by the insert of polished graphite. Such insert also provides creation of artificial centers of bubbles formation uniformly distributed on the entire selected evaporator

surface. The dependencies of thicknesses on evaporation time for $As_2Se_3(1)$ and $As_2S_3(2)$ layers on a fixed substrate at the corresponding temperatures providing the bubble mechanism of material heating up in the evaporator are given in Fig.5. The linear $d=f(t)$ dependency shows a constant rate of CGS material evaporation.

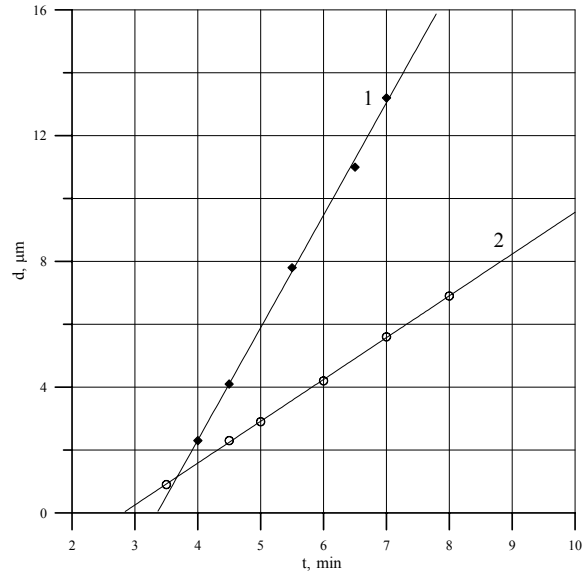


Fig.5. The dependencies of thicknesses on evaporation time for $As_2Se_3(1)$ and $As_2S_3(2)$ layers on a fixed substrate.

The evaporators with the activated surface proved to be good for the evaporation of As_2S_3 plasticized with (1-3) at.% Sn. At the evaporation from the metallic evaporator the given material in the literal sense “get out” from the evaporator, makes it difficult to obtain the reproducible results. If to activate the metallic evaporator surface by a pyroceram platen placed with the rough (back) side to CGS material, then on the account of big amount of the bubble centers generation compared to the case of the polished graphite the process of As_2S_3 plasticized with Sn becomes stable. But on the account of the further decrease of the evaporator free energy the evaporation rate decreases somewhat and the obtained films possess the reproducible electro-physical properties.

2.3 Preparation of CGS thin films on a flexible substrate

The proposed open type evaporators with the activated surface can be used for the preparation of CGS films on the long flexible lavsan ribbons. But the amount of the ribbon with CGS is limited by the evaporator volume, its high thermal inertia needed for uniform CGS warming-up per the length unit of the semiconductor layer due to accumulation in the evaporator of CGS remains having none-uniform composition of the molecular vapor in the bubbles.

The method of multiple coatings for the preparation of CGS films on the long lavsan ribbons by using the open type evaporators is described in the paper [16]. The long CGS with averaging electro-physical parameters were obtained. By on the account of tribo adhesion during a multiple substrate passing over the evaporator the appearing defects inside of CGS films sharply decrease the carrier quality, which especially has an impact at holographic recording.

Using of the flash evaporation method for the fabrication of CGS layers in the form of long ribbons it is impossible due to high evaporator temperature as at the method is based on a postulate: the rate of material supply should equal the rate of its evaporation. For the obtaining of the extended homogeneous CGS layers with the constant and reproducible parameters we suggested to use an interconnected system: batcher-extended evaporator. The given system provides a periodical supply of the entire surface of the heated up evaporator with the small portions of the evaporated material, which in the evaporator are on their evaporation time interval and on their geometrical segment of the evaporator. The supply periodicity of every regular segment of the evaporator requires the entrance in an operating mode of the preliminary loaded portion, then in every moment of time the total molecular flow will contain the whole composition of the molecular vapor and its density corresponds to the evaporation of a single dose of the initial CGS. The condensation zone is optimized for specific vacuum equipment. As the molecular flow distribution from each dose being on its time segment of evaporation is subjected to the kossinus law, then the increase of α_R angle leads to the molecular flow decrease.

The number of the evaporated doses during the motion of the allotted substrate segment in the condensation zone provides the given thickness and stability of the CGS film electro-physical parameters. The loading periodicity is provided by the batcher on the shaft of which the wells of same volume are situated shifted relative to one another on an angle of $180^\circ/n$ (where n – is the number of the evaporated doses) and distributed along the evaporator length, that determines the evaporator length. The evaporation is carried out by using calibrated CGS grains, which are loaded in the batcher bunker which provides the same heat up time for the dose feed to the evaporator. In all cases the evaporation temperature corresponds to the bubble boiling of the given CGS and the evaporator heat inertia is sufficient for the evaporated doses not to influence on its temperature.

2.4 The estimation of the quality of CGS films.

The comparative analysis of two methods of As_2S_3 film preparation were presented as the given material according to [10] is evaporated congruently. In the first case an evaporator with the activated surface was used and after its access to the operating mode the metallized on the both sides lavsan basis was chased away in both direction a few times. In the second case the batcher – evaporator system was used and the film thickness was

turned out during a single chase out. From the studies of As_2S_3 layers surface by a scanning probe microscope of Nanoscope VEECO type it was established that in both cases the film thickness is the same and equals $1.5 \mu m$. From the comparison of As_2S_3 films surface (Fig.6) one can see that at the multiple chase out the layers inhomogeneity makes $\approx 75 nm$. For a single chase out the As_2S_3 layers surface inhomogeneity decreases to $40 nm$. In the first case the strongly marked surface inhomogeneities could be explained by the appearance of the defects on the CGS surface due to tribo-adhesion, which provides additional centers of the film growth. In the second case the surface inhomogeneity is mainly determined by the inhomogeneity of the metallized lavsan basis.

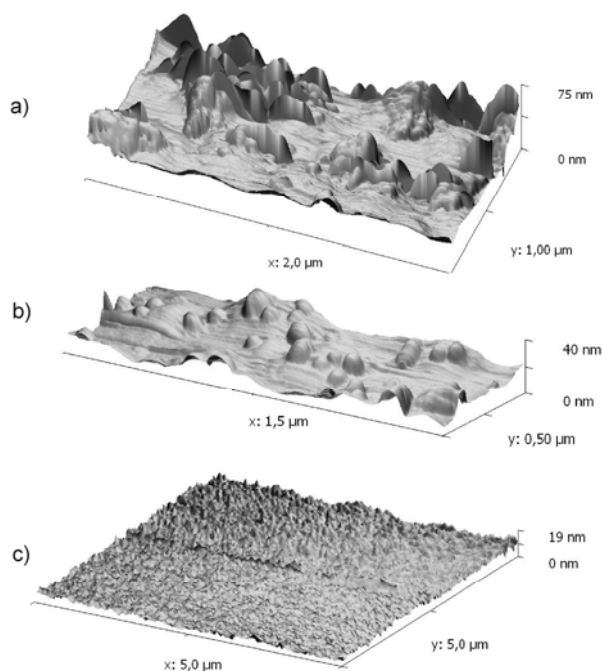


Fig.6. Images of the layer surface: a) As_2S_3 film obtained by multiple depositions; b) As_2S_3 film obtained by single deposition; c) thermoplastic films on As_2S_3 .

The electro-physical parameters of As_2S_3 films and of the compound materials such as $As_4S_3Se_3$ (92 mol%) + As_2S_3 (8 mol%), which further is designated as $As_4S_3Se_3 + As_2S_3$, were studied. The films obtained at the deposition of $As_4S_3Se_3$ solid solutions were studied separately. The spectral distribution of CGS films was studied by a standard method and as a front electrode the conductive glue deposited through a stencil-plate was used. The photoconductivity maximum was estimated as the ratio (I_{ph}/P) (A/W) of the maximum photocurrent (I_{ph}) to the incident light flow power unit (P). The photographic sensitivity (S_{ph}) of CGS films was estimated by the potential decline in the recording mode at the illumination by integral light ($E=0.6 lx$). The parameters of the prepared CGS films are given in the Table 1 below.

Table 1. Parameters of CGS films obtained at multiple and single chase-out

Nr	Composition	d, μm	λ_{max} , nm	(I_{it}/P) (A/W)	$S_{\text{ph}, \text{lx}^{-1} \cdot \text{s}^{-1}}$
1	As ₂ S ₃ multiple	1.3	456	$1.5 \cdot 10^{-6}$	0.07
2	As ₂ S ₃ single	1.3	456	$8.0 \cdot 10^{-6}$	0.09
3	As ₄ S ₃ Se ₃ + As ₂ S ₃ multiple	1.3	538	$4.0 \cdot 10^{-5}$	0.12
4	As ₄ S ₃ Se ₃ + As ₂ S ₃ single	1.3	540	$1.4 \cdot 10^{-4}$	0.17
5	As ₄ S ₃ Se ₃ multiple	1.3	572	$1.2 \cdot 10^{-5}$	0.18
6	As ₄ S ₃ Se ₃ single	1.3	564	$8.0 \cdot 10^{-3}$	0.23

As one can see from the Table 1 in all cases the photosensitivity of CGS films obtained by the technology of the single chase out is higher relative to multiple chase out. Besides for the estimation of CGS layers quality the photo-thermoplastic carriers were created by depositing on a semiconductor surface of a thermoplastic layer consisting of a polymer solution in toluene. The low values of polymer layer thickness allow more relief to reveal the CGS layer defects. The photo-thermoplastic carriers based on CGS As₄S₃Se₃+ As₂S₃ semiconductor and poly-N-epoxypropylcarbazole with a thickness of 0.3 μm were obtained. The AFM images of a diffraction grating surface, recorded at a spatial recording frequency $\nu=3500 \text{ mm}^{-1}$ are brought in Fig.7.

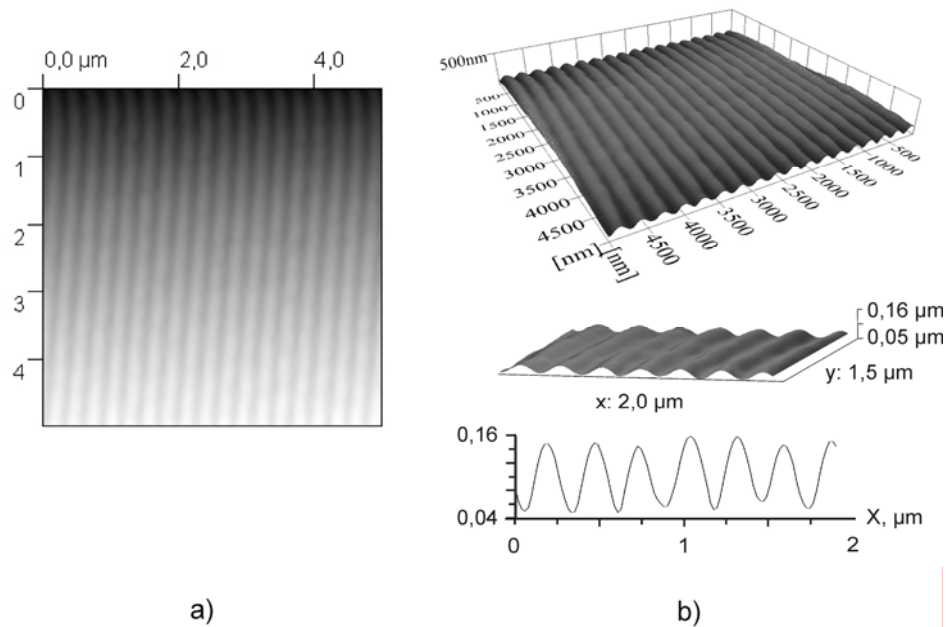


Fig.7. a) PTP carrier surface image at $\nu=3500 \text{ mm}^{-1}$; b) profile depth of the diffraction grating.

As one can see from Fig.7 the diffraction grating consists of rectilinear grooves without presence of visible defects or distortions. The average deformation profile depth makes around 0.11 μm . The annealing temperature influences significantly the properties of the chalcogenide films prepared by different methods (see for example [17]).

3. Conclusions

The bubble mechanism of CGS material warmed-up in the evaporator leads to the homogeneous character of the evaporation-condensation of the evaporated material. The activation of the open type evaporator surface leads to the generation of the CGS bubbles on the entire evaporator surface, which allows to get CGS films with the stable electro-physical properties. Using of a batcher-evaporator system allows to obtain homogeneous CGS films onto a long flexible substrate.

References

- [1] S. N. Agbo, P. E. Ugwuoke, F. I. Ezema, Journal of Ovonic Research, **8**(4), 81 (2012).
- [2] T. EL Ashram, M. Kamal, A. Raouf, S. Mosaad, Journal of Ovonic Research, **8**(4), 97 (2012).
- [3] D. Kathirvel, N. Suriyanarayanan, S. Prabakar, S. Srtikanth, Journal of Ovonic Research, **7**(4), 83 (2011).
- [4] Neha Shjartma, Sunanda Sharda, Vineet Sharma, Pankaj Sharma, Chalcogenide Letters **9**(8), 335 (2012).
- [5] Mohammad Istiaque Hossain, Chalcogenide Letters, **9**(6), 231 (2012).
- [6] J. Santos Cruz, S. A. Mayen Hernandez, J. Coronel Hernandez, R. Mejia Rodriguez, R. Castanedo Perez, G. Torresw Delgado, S. Jimenez Sandoval, Chalcogenide Letters **9**(2), 85 (2012).

- [7] P. Usha Rajalakshmi, Fachel Oommen, C. Sasnjeeviraja, Chalcogenide Letters, **8**(11), 683 (2011)
- [8] N. Jessy Mathew, Rachel Oommen, Usha Rajalakshmi, P. C. Sanjeeviraja, Chalcogenide Letters, **8**(7), 441 (2011).
- [9] X. Zheng, H. Tao, F. Cherng, H. Guo, C. Lin, X. Zhao Chalcogenide Letters, **8**(6), 371 (2011).
- [10] Poltavtsev Iu.G. Semiconductors structure in the none-crystalline state (in Russian). Advances of Physical Sciences, **120**, 581 (1976).
- [11] Panasiuc L.M. Peculiarities of glassy arsenic chalcogenides evaporation kinetics (in Russian), Scientific Annals of the SUM , series “Physical and mathematical Sciences”, Chisinau, 2001, pp.159-161.
- [12] Novoselova A.V. Vapor pressure of the volatile chalcogenide metals (in Russian). Moscow, Science,1978
- [13] Nesis E.I. The liquid boiling (in Russian). Moscow, Science,1973.
- [14] Petuhov B.S.,Geshin L.G.,Kovalev S. A., Heat transfer in the nuclear energy installations (in Russian). Moscow. Atomic publishing house, 1974
- [15] Certificate of authorship., 4022 MD .Evaporator. (MD), 2010
- [16] V.M. Yishimov, E.A. Senokosov, I. V. Dementiev, T.I Goglidze, Technical .Phys. Letters. **28**(16), 79 (2002) (in Russian)
- [17] A. A. Abu-Sehly, A.A. Elabbar, Digest J. Nanomat.Biostructures **7**(2), 763 (2012).

*Corresponding author: mihaip58@yahoo.com